

# Spawning Models for the CPHD Filter

Daniel S. Bryant, Emmanuel D. Delande, Steven Gehly, Jérémie Houssineau, Daniel E. Clark, Brandon A. Jones

**Abstract**—In its classical form, the Cardinalized Probability Hypothesis Density (CPHD) filter does not model the appearance of new targets through spawning, yet there are applications for which spawning models more appropriately account for newborn objects when compared to spontaneous birth models. In this paper, we propose a principled derivation of the CPHD filter with spawning from the Finite Set Statistics framework. A Gaussian Mixture implementation of the CPHD filter with spawning is then presented, illustrated with three applicable spawning models on a simulated scenario involving two parent targets spawning a total of five objects. Results show that filter implementations with spawn models provide more accurate results when compared to a birth model implementation.

**Index Terms**—Multi-object Filtering, CPHD Filter, Point Processes, Random Finite Sets, Bayesian Estimation, Target Tracking, Target Spawning

## I. INTRODUCTION

THE goal of the multi-object estimation problem is to jointly estimate – usually in the presence of clutter, data association uncertainty, and missed detections – the time-varying number and individual states of targets evolving in a surveillance scene. Commonly known detection and tracking algorithms for the multi-object problem include Joint Probabilistic Data Association (JPDA) [1] and Multiple Hypothesis Tracking (MHT) [2]. Relatively new is the multi-object filtering framework known as Finite Set Statistics (FISST) [3], [4], based on a representation of the target population as a Random Finite Set (RFS), a specific case of the more general concept of point process.

Within the FISST framework, the multi-target Bayes filter proposes an optimal solution to the multi-object estimation problem; it is, however, impractical in realistic applications due to its combinatorial complexity [3]. Several approximations of the multi-target Bayes filter have been proposed to circumvent this intractability, including the Probability Hypothesis Density (PHD) [5] and the Cardinalized Probability Hypothesis Density (CPHD) [6] filters. The PHD filter propagates the first-order factorial moment density, or *intensity*, of the multi-target RFS, representing the whole population of targets within the surveillance scene [5]. While inexpensive, the PHD filter exhibits a high variability in the estimated target number [4]. The CPHD filter [6] addresses this issue by estimating the cardinality distribution of the multi-target RFS in addition to its intensity. Unlike for the PHD filter, the initial

presentation of the CPHD filter does not include a model for target spawning. Target spawning refers to instances where a parent target generates one or more daughter targets and where the daughter(s) usually remain(s) in close proximity to the parent for some amount of time following their appearance, e.g., a fighter jet that launches a missile.

Though the CPHD filter's model for birth targets has the potential to address spawning targets [4], there may be cases where specific spawning models are more applicable. In the context of the tracking of Resident Space Objects (RSOs), natural and artificial Earth orbiting satellites consisting of active spacecraft, decommissioned payloads, and debris, consider for example the deployment of CubeSats from a launch vehicle [7], [8] or fragmentation events caused by the unintentional [9] or intentional [10] collision of objects. Without spawning, the best option may be the use of diffuse birth regions, however, the volume of space to be filled requires a potentially intractable number of birth regions [11]. To improve the CPHD filter's performance for space-object tracking, [12] presented a measurement-based birth model that leverages an astrodynamics approach to track initialization for RSOs. While such an approach may be effective for tracking spawned RSOs, a multi-target filter that correctly models the birth process for a given target is expected to provide better accuracy and faster confirmation of new objects. The models proposed in this paper allow for the development of CPHD implementations used for RSO tracking applications with spawning.

The incorporation of spawning models in the context of CPHD filtering has previously been explored in [13], relying on an intuitive construction of the filtering equations related to the spawning models considered (Bernoulli or Poisson process) through a non-standard derivation procedure. In this paper, we propose expressions for the CPHD filter enhanced with various target spawning models through a standard derivation procedure within the FISST framework specific to the considered spawning model (Bernoulli, Poisson, or zero-inflated Poisson process). To the best of our understanding, the derivation of the spawning terms in [13] relies on additional approximations and the approach does not lead to the same results as those presented here.

The structure of this paper is as follows. Section II presents the relevant background on point processes and functional differentiation, followed by key definitions and properties pertinent to our results. Section III provides a detailed construction of the CPHD filter with target spawning, considering several models of spawning processes. Section IV demonstrates the proposed concepts through simulation example, and closing remarks are given in Section V. The proofs of the results in Section III are given in the Appendix.

D. S. Bryant, S. Gehly, and B. A. Jones are with the Department of Aerospace Engineering Sciences, University of Colorado Boulder, Boulder, CO 80309 USA (e-mail: daniel.bryant@colorado.edu; steven.gehly@colorado.edu; brandon.jones@colorado.edu)

E. D. Delande, J. Houssineau, and D. E. Clark are with the School of Engineering and Physical Sciences, Heriot-Watt University (HWU), Edinburgh EH14 4AS, U.K. (e-mail: E.D.Delande@hw.ac.uk; j.houssineau@hw.ac.uk; d.e.clark@hw.ac.uk)

## II. BACKGROUND

In this section, we introduce the necessary background on point processes (Section II-A), on Probability Generating Functional (p.g.fl.)s (Section II-B), on functional differentiation (Section II-C), and on a few properties from the application of differentiation in the context of point processes (Section II-D).

### A. Point processes

A point process on some space  $\mathbf{X}$  is a random variable whose number of elements *and* element states, belonging to  $\mathbf{X}$ , are random. In the context of multi-target tracking the population of targets is represented by a point process  $\Phi$ , on a single-target state space  $\mathbf{X} \subseteq \mathbb{R}^d$ , whose elements describe individual target states. A realization of  $\Phi$  is a vector of points  $\varphi = (x_1, \dots, x_N)$  depicting a specific multi-target configuration, where  $x_i \in \mathbf{X}$  describes the  $d$ -component state of an individual target (position, velocity, etc.).

A point process  $\Phi$  is characterized by its probability distribution  $P_\Phi$  on the measurable space  $(\mathcal{X}, \mathbf{B}_\mathcal{X})$ , where  $\mathcal{X} = \bigcup_{n \geq 0} \mathbf{X}^n$  is the point process state space, i.e., the space of all the finite vectors of points in  $\mathbf{X}$ , and  $\mathbf{B}_\mathcal{X}$  is the Borel  $\sigma$ -algebra on  $\mathcal{X}$  [14]. The probability distribution of a point process is defined as a symmetric function, so that the order of points in a realization is irrelevant for statistical purposes – for example, realizations  $(x_1, x_2)$  and  $(x_2, x_1)$  are equally probable. In addition, if the probability distribution is such that the realizations are vectors of points that are pairwise distinct *almost surely*, then the point process is called *simple*. For the rest of the paper, all the point processes are assumed simple<sup>1</sup>.

The probability distribution  $P_\Phi$  is characterized by its projection measures  $P_\Phi^{(n)}$ , for any  $n \geq 0$ . The  $n^{\text{th}}$ -order projection measure  $P_\Phi^{(n)}$ , for any  $n \geq 1$ , is defined on the Borel  $\sigma$ -algebra of  $\mathbf{X}^n$  and gives the probability for the point process to be composed of  $n$  points, and the probability distribution of these points. By extension,  $P_\Phi^{(0)}$  is the probability for the point process to be empty. For any  $n \geq 0$ ,  $J_\Phi^{(n)}$  denotes the  $n^{\text{th}}$ -order Janossy measure [16, p. 124], and is defined as

$$J_\Phi^{(n)}(B_1 \times \dots \times B_n) = \sum_{\sigma(n)} P_\Phi^{(n)}(B_{\sigma_1} \times \dots \times B_{\sigma_n}) \quad (1a)$$

$$= n! P_\Phi^{(n)}(B_1 \times \dots \times B_n), \quad (1b)$$

where  $B_i$  is in  $\mathbf{B}_\mathbf{X}$ , the Borel  $\sigma$ -algebra of  $\mathbf{X}$ ,  $1 \leq i \leq n$ , and where  $\sigma(n)$  denotes the set of all permutations  $(\sigma_1, \dots, \sigma_n)$  of  $(1, \dots, n)$ .

The probability density  $p_\Phi$  (respectively (resp.) the  $n^{\text{th}}$ -order projection density  $p_\Phi^{(n)}$ , the  $n^{\text{th}}$ -order Janossy density  $j_\Phi^{(n)}$ ) is the Radon-Nikodym derivative of the probability distribution  $P_\Phi$  (resp. the  $n^{\text{th}}$ -order projection measure  $P_\Phi^{(n)}$ , the  $n^{\text{th}}$ -order Janossy measure  $J_\Phi^{(n)}$ ) with respect to (w.r.t.) some reference measure. All these quantities provide equivalent

ways to describe the point process  $\Phi$ . However, a measure-theoretical formulation provides a more general framework that is required to construct certain statistical properties on point processes that can be exploited for practical applications; a recent example is given in [17] for the construction of the regional statistics. For the sake of generality, the rest of the paper thus uses a measure-based description.

Assuming that  $f$  is a non-negative measurable function on  $\mathcal{X}$ , then the integral of  $f$  w.r.t. to the measure  $P_\Phi$  can be written in the following ways:

$$P_\Phi(f) = \int_{\mathcal{X}} f(\varphi) P_\Phi(d\varphi) \quad (2a)$$

$$= \int_{\mathcal{X}} f(\varphi) p_\Phi(\varphi) d\varphi \quad (2b)$$

$$= \sum_{n \geq 0} \int_{\mathbf{X}^n} f(x_1, \dots, x_n) P_\Phi^{(n)}(d(x_1, \dots, x_n)) \quad (2c)$$

$$= \sum_{n \geq 0} \int_{\mathbf{X}^n} f(x_1, \dots, x_n) p_\Phi^{(n)}(x_1, \dots, x_n) dx_1 \dots dx_n \quad (2d)$$

$$= \sum_{n \geq 0} \frac{1}{n!} \int_{\mathbf{X}^n} f(x_1, \dots, x_n) J_\Phi^{(n)}(d(x_1, \dots, x_n)) \quad (2e)$$

$$= \sum_{n \geq 0} \frac{1}{n!} \int_{\mathbf{X}^n} f(x_1, \dots, x_n) j_\Phi^{(n)}(x_1, \dots, x_n) dx_1 \dots dx_n. \quad (2f)$$

Throughout this article the exploitation of the Janossy measures will be preferred, for they are convenient tools in the context of functional differentiation (see Section II-C). For the sake of simplicity, domains of integration will be omitted when they refer to the full target state space  $\mathbf{X}$ .

The Janossy measures can also be used directly to exploit meaningful information on the point process  $\Phi$ . For example, central to this article is the extraction of the *cardinality distribution*  $\rho_\Phi$  of the point process, that describes the number of elements in the realizations of  $\Phi$  (see Section III):

**Example 1** (Cardinality distribution). *Consider the function  $f_n$  defined as*

$$f_n(\varphi) = \begin{cases} 1, & |\varphi| = n, \\ 0, & \text{otherwise,} \end{cases} \quad (3)$$

where  $|\varphi|$  denotes the size of the vector  $\varphi$ . The integral of  $f_n$  w.r.t. to  $P_\Phi$  yields the probability  $\rho_\Phi(n)$  that a realization  $\varphi$  of the point process  $\Phi$  has size  $n$  and we have, using Eq. (2) (see [18, p.28]):

$$\rho_\Phi(n) = P_\Phi(f_n) \quad (4a)$$

$$= \int_{\mathbf{X}^n} P_\Phi^{(n)}(d(x_1, \dots, x_n)) \quad (4b)$$

$$= \frac{1}{n!} \int_{\mathbf{X}^n} J_\Phi^{(n)}(d(x_1, \dots, x_n)). \quad (4c)$$

The function  $\rho_\Phi$  is called the *cardinality distribution* of the point process  $\Phi$ . Note that the  $n^{\text{th}}$ -order projection measure  $P_\Phi^{(n)}$  (resp. the  $n^{\text{th}}$ -order Janossy measure  $J_\Phi^{(n)}$ ) is not a

<sup>1</sup>An alternative construction of simple point processes as random objects whose realizations are *sets* of points  $\varphi = \{x_1, \dots, x_N\}$ , in which the elements are per construction *unordered*, is also available in the literature [6], [15]. In this context, a point process is called a RFS.

probability measure, in the general case, for its integral over  $\mathbf{X}^n$  yields  $\rho_\Phi(n)$  (resp.  $n!\rho_\Phi(n)$ ).

### B. Probability generating functionals

The p.g.fl. provides a useful characterization for point process theory [19] and is defined as follows.

**Definition 1** (Probability generating functional [16]). *The probability generating functional  $G_\Phi$  of a point process  $\Phi$  on  $\mathbf{X}$  can be written for any test function  $h \in \mathcal{U}(\mathbf{X})$  as<sup>2</sup>*

$$\begin{aligned} G_\Phi(h) &= \int_{\mathcal{X}} \left[ \prod_{x \in \varphi} h(x) \right] P_\Phi(d\varphi) \\ &= J_\Phi^{(0)} + \sum_{n \geq 1} \frac{1}{n!} \int_{\mathbf{X}^n} h(x_1) \dots h(x_n) J_\Phi^{(n)}(d(x_1, \dots, x_n)). \end{aligned} \quad (5a)$$

$$(5b)$$

The p.g.fl.  $G_\Phi$  fully characterizes the point process  $\Phi$ , and is a very convenient tool for the extraction of statistical information on  $\Phi$  through functional differentiation (see Section II-C). From Eq. (5) we can immediately write

$$G_\Phi(0) = J_\Phi^{(0)} (= P_\Phi^{(0)}), \quad (6)$$

$$G_\Phi(1) = 1. \quad (7)$$

Operations on point processes (e.g., superposition of two populations) can be translated into operations on their corresponding p.g.fl.s. In the context of multi-target tracking, p.g.fl.s provide a convenient description of the compound population (targets or measurements) resulting from an operation on elementary populations.

The superposition operation for point processes describes the union of two populations  $\Phi_1, \Phi_2$  into a compound population  $\Phi_1 \cup \Phi_2$ , during which the information about the origin population of each individual is lost.

**Proposition 1** (Superposition of independent processes [19]). *Let  $\Phi_1$  and  $\Phi_2$  be two independent point processes defined on the same space, with respective p.g.fl.s  $G_{\Phi_1}$  and  $G_{\Phi_2}$ . The p.g.fl. of the superposition process  $\Phi_1 \cup \Phi_2$  is given by the product*

$$G_{\Phi_1 \cup \Phi_2}(h) = G_{\Phi_1}(h)G_{\Phi_2}(h). \quad (8)$$

The Galton-Watson recursion for point processes [19], [20] describes the evolution of each individual  $x$  from a parent population  $\Phi_p$  into a population of daughter individuals, independently of the other parent individuals but following a common evolution model described by a process  $\Phi_e$ . The resulting daughter population  $\Phi_d$  is then the superposition of all the populations of daughter individuals.

**Proposition 2** (The Galton-Watson recursion [20]). *Let  $G_{\Phi_p}$  be the p.g.fl. of a parent process  $\Phi_p$  on  $\mathbf{X}$ , and let  $G_{\Phi_e}(\cdot|x)$  be the conditional p.g.fl. of an evolution process  $\Phi_e$ , defined for every  $x \in \mathbf{X}$ . The p.g.fl. of the daughter process  $\Phi_d$  is given by the composition*

$$G_{\Phi_d}(h) = G_{\Phi_p}(G_{\Phi_e}(h|\cdot)). \quad (9)$$

<sup>2</sup> $\mathcal{U}(\mathbf{X})$  is the space of bounded measurable functions  $u$  on  $\mathbf{X}$  satisfying  $\|u\|_\infty \leq 1$ .

### C. Functional differentiation

To make use of functionals in the derivations presented in Section III, we require the notion of differentials on functional spaces. We adopt a restricted form of the Gâteaux differential, known as the chain differential [21], so that a general chain rule can be determined [22], [23]. Following this, we describe the general higher-order chain rule.

**Definition 2** (Chain differential [21]). *Under the conditions detailed in [21], the function  $f$  on some set  $X$  has a chain differential  $\delta f(x; \eta)$  at  $x \in X$  in the direction  $\eta$  if, for any sequence  $\eta_n \rightarrow \eta \in X$ , and any sequence of real numbers  $\theta_n \rightarrow 0$ , it holds that*

$$\delta f(x; \eta) = \lim_{n \rightarrow \infty} \frac{1}{\theta_n} (f(x + \theta_n \eta_n) - f(x)). \quad (10)$$

The  $n^{\text{th}}$ -order chain differential can be defined recursively as

$$\delta^n f(x; \eta_1, \dots, \eta_n) = \delta(\delta^{n-1} f(x; \eta_1, \dots, \eta_{n-1}); \eta_n). \quad (11)$$

Applying  $n^{\text{th}}$ -order chain differentials on composite functions can be an extremely laborious process since it involves determining the result for each choice of function and proving the result by induction. For ordinary derivatives, the general higher-order chain rule is normally attributed to Faà di Bruno [24]. The following result generalizes Faà di Bruno's formula to chain differentials and allows for a systematic derivation of composite functions (see [22] for an example of exploitation in the context of Bayesian estimation).

**Proposition 3** (General higher-order chain rule, from [23], [25]). *Under the differentiability and continuity conditions detailed in [25], the  $n^{\text{th}}$ -order variation of composition  $f \circ g$  in the sequence of directions  $(\eta_i)_{i=1}^n$  at point  $x$  is given by*

$$\begin{aligned} \delta^n (f \circ g)(x; (\eta_i)_{i=1}^n) \\ = \sum_{\pi \in \Pi_n} \delta^{|\pi|} f \left( g(x); \left( \delta^{|\omega|} g(x; (\eta_i)_{i \in \omega}) \right)_{\omega \in \pi} \right), \end{aligned} \quad (12)$$

where  $\Pi_n = \Pi(\{1, \dots, n\})$  represents the set of partitions of the index set  $\{1, \dots, n\}$ , and  $|\pi|$  denotes the cardinality of the set  $\pi$ .

**Example 2** (General higher-order chain rule).

$$\begin{aligned} \delta^2 (f \circ g)(x; \eta_1, \eta_2) \\ = \underbrace{\delta^2 f(g(x); \delta g(x; \eta_1), \delta g(x; \eta_2))}_{\pi = \{\{1\}, \{2\}\}} + \underbrace{\delta f(g(x); \delta^2 g(x; \eta_1, \eta_2))}_{\pi = \{\{1, 2\}\}}. \end{aligned} \quad (13)$$

Applying  $n^{\text{th}}$ -order chain differentials on a product of functions follows a more straightforward approach, similar to Leibniz' rule for ordinary derivatives.

**Proposition 4** (Leibniz' rule, from [25]). *Under the differentiability conditions detailed in [25], the  $n^{\text{th}}$ -order variation of*

the product  $f \cdot g$  in the sequence of directions  $(\eta_i)_{i=1}^n$  at point  $x$  is given by

$$\begin{aligned} \delta^n(f \cdot g)(x; (\eta_i)_{i=1}^n) \\ = \sum_{\pi \subseteq \{1, \dots, n\}} \delta^{|\pi|} f(x; (\eta_i)_{i \in \pi}) \delta^{n-|\pi|} g(x; (\eta_i)_{i \in \pi^c}), \end{aligned} \quad (14)$$

where  $\pi^c = \{1, \dots, n\} \setminus \pi$  denotes the complement of  $\pi$  in  $\{1, \dots, n\}$ .

**Example 3** (Leibniz' rule).

$$\begin{aligned} \delta^2(f \cdot g)(x; \eta_1, \eta_2) = \\ \underbrace{\delta^2 f(x; \eta_1, \eta_2) g(x)}_{\pi=\{1,2\}} + \underbrace{\delta f(x; \eta_1) \delta g(x; \eta_2)}_{\pi=\{1\}} \\ + \underbrace{\delta f(x; \eta_2) \delta g(x; \eta_1)}_{\pi=\{2\}} + \underbrace{f(x) \delta g(x; \eta_1, \eta_2)}_{\pi=\{\emptyset\}}. \end{aligned} \quad (15)$$

#### D. Probability generating functionals and differentiation

Key properties of a point process can be recovered from the functional differentiation of its p.g.fl.. Taking the  $k^{\text{th}}$ -order variation of  $G_\Phi(h)$  in the directions  $\eta_1, \dots, \eta_k$ , we have (see, for example [26, p. 21]),

$$\begin{aligned} \delta^k G_\Phi(h; \eta_1, \dots, \eta_k) = \\ \sum_{n \geq k} \frac{1}{(n-k)!} \int_{\mathbf{X}^n} \prod_{i=1}^k \eta_i(x_i) \prod_{i=k+1}^n h(x_i) J_\Phi^{(n)}(d(x_1, \dots, x_n)). \end{aligned} \quad (16)$$

It is then useful to consider the cases when we set  $h = 1$  or  $h = 0$ , i.e.

$$\begin{aligned} \delta^k G_\Phi(0; \eta_1, \dots, \eta_k) \\ = \int_{\mathbf{X}^k} \eta_1(x_1) \dots \eta_k(x_k) J_\Phi^{(k)}(d(x_1, \dots, x_k)), \end{aligned} \quad (17)$$

$$\begin{aligned} \delta^k G_\Phi(1; \eta_1, \dots, \eta_k) \\ = \int_{\mathbf{X}^k} \eta_1(x_1) \dots \eta_k(x_k) M_\Phi^{(k)}(d(x_1, \dots, x_k)), \end{aligned} \quad (18)$$

where  $M_\Phi^{(k)}$  is the  $k^{\text{th}}$ -order factorial moment measure, defined as in [14, p. 111].

Assuming that one wishes to evaluate the Janossy and factorial moment measures in some measurable subsets  $B_i \in \mathbf{B}_\mathbf{X}$ ,  $1 \leq i \leq k$ , then they can be recovered from Eqs (17), (18) by setting the directions to be indicator functions<sup>3</sup>  $\eta_i = 1_{B_i}$ ,  $1 \leq i \leq k$ , so that

$$\delta^k G_\Phi(h; 1_{B_1}, \dots, 1_{B_k})|_{h=0} = J_\Phi^{(k)}(B_1 \times \dots \times B_k), \quad (19)$$

$$\delta^k G_\Phi(h; 1_{B_1}, \dots, 1_{B_k})|_{h=1} = M_\Phi^{(k)}(B_1 \times \dots \times B_k). \quad (20)$$

The propagation of the first-order factorial moment measure  $M_\Phi^{(1)}$  – also called the *intensity measure*  $\mu_\Phi$  – of the multi-target point process  $\Phi$ , in a Bayesian context, is a key component of the construction of both the PHD filter [5] and the CPHD filter [6]. The density of the intensity measure is called the *Probability Hypothesis Density* [5].

<sup>3</sup>For a measurable subset  $B \in \mathbf{B}_\mathbf{X}$ , the indicator function  $1_B$  is defined as the function on  $\mathbf{X}$  such that  $1_B(x) = 1$  if  $x \in B$ ,  $1_B(x) = 0$  otherwise.

### III. THE CPHD FILTER WITH SPAWNING

This section covers the derivation of the filtering equations for the CPHD filter for various target spawning processes. Section III-A provides a brief description of the general multi-target Bayes filter [3], and the principled approximation leading to the construction of the original CPHD filter [6]. Section III-B then presents the various models of point processes that will be necessary for the construction of the CPHD filter with spawning in Section III-C.

#### A. Multi-object filtering and CPHD filter

The multi-target Bayes filter [3] is the natural extension of the usual single-target Bayesian paradigm to the multi-target case, within the FISST framework. The multi-target Bayes recursion at time step  $k$  consists of the *time prediction* and *data update* steps given as follows:

$$P_{k|k-1}(d\varphi|Z_{1:k-1}) = \int_{\mathcal{X}} f_{k|k-1}(\varphi|\bar{\varphi}) P_{k-1}(d\bar{\varphi}|Z_{1:k-1}), \quad (21)$$

$$P_k(d\varphi|Z_{1:k}) = \frac{g_k(Z_k|\varphi) P_{k|k-1}(d\varphi|Z_{1:k-1})}{\int_{\mathcal{X}} g_k(Z_k|\bar{\varphi}) P_{k|k-1}(d\bar{\varphi}|Z_{1:k-1})}, \quad (22)$$

where  $P_{k|k-1}$  (resp.  $P_k$ ) is the probability distribution of the predicted multi-target process  $\Phi_{k|k-1}$  (resp. the posterior multi-target process  $\Phi_k$ ),  $Z_i$ ,  $1 \leq i \leq k$ , is the set of measurements collected at time step  $i$ ,  $Z_{1:i}$  denotes the sequence  $Z_1, \dots, Z_i$ ,  $f_{k|k-1}$  is the multi-target transition kernel, and  $g_k$  is the multi-target likelihood function. The multi-target transition kernel  $f_{k|k-1}$  describes the time evolution of the population of targets since time step  $k-1$  and encapsulates the underlying models of target birth, motion, spawning, and death. The multi-target likelihood  $g_k$  describes the sensor observation process and encapsulates the underlying models of target detection, target-generated measurements, and false alarms.

The multi-target Bayes recursion is used to propagate the posterior distribution  $P_k(\cdot|Z_{1:k})$  that describes the current target population based on all the measurements  $Z_1, \dots, Z_k$  collected so far. The CPHD Bayes recursion aims at simplifying the multi-target Bayes recursion by approximating the predicted and posterior multi-target processes as independent and identically distributed (i.i.d.) processes<sup>4</sup>, a class of point processes fully characterized by their cardinality distribution  $\rho_\Phi$  and their first-order moment measure  $\mu_\Phi$  [6]. The CPHD filter thus focuses on the propagation of the posterior cardinality distribution  $\rho_k$  and the posterior first-order moment measure  $\mu_k$ , rather than the full posterior probability distribution  $P_k$ .

The original construction of the CPHD filter [6] does not consider a target spawning mechanism, and the key contribution of this paper is to propose the integration of several target spawning models in the CPHD time prediction equation (see Section III-C). Note that the data update step does not involve the target spawning mechanism and is therefore left out of the scope of this paper. A detailed description of the data update step can be found in [27].

<sup>4</sup>The definition of an i.i.d. process is given in Section III-B.



### B. Point process models

1) *Bernoulli process*: A Bernoulli process  $\Phi$  is characterized by a parameter  $0 \leq p \leq 1$  and a spatial distribution  $s$ . It describes the situation where 1) either there is no object in the scene, or 2) there is a single object in the scene, with state distributed according to  $s$ . Its projection measures are given by

$$P_{\Phi}^{(n)}(B_1 \times \dots \times B_n) = \begin{cases} 1 - p, & n = 0, \\ ps(B_1), & n = 1, \\ 0, & \text{otherwise.} \end{cases} \quad (23)$$

**Proposition 5** (p.g.fl. of a Bernoulli process [4]). *The p.g.fl. of a Bernoulli process  $\Phi$  with parameter  $p$  and spatial distribution  $s$  is given by*

$$G_{\Phi}(h) = 1 - p + p \int h(x)s(dx). \quad (24)$$

2) *Poisson process*: A Poisson process  $\Phi$  is characterized by a rate  $\lambda \geq 0$  and a spatial distribution  $s$ . It describes a population whose size follows a Poisson distribution and whose individual states are i.i.d. according to  $s$ . Its projection measures are given by

$$P_{\Phi}^{(n)}(B_1 \times \dots \times B_n) = e^{-\lambda} \frac{\lambda^n}{n!} \prod_{i=1}^n s(B_i). \quad (25)$$

**Proposition 6** (p.g.fl. of a Poisson process [4]). *The p.g.fl. of a Poisson process  $\Phi$  with rate  $\lambda$  and spatial distribution  $s$  is given by*

$$G_{\Phi}(h) = \exp \left[ \lambda \left( \int h(x)s(dx) - 1 \right) \right]. \quad (26)$$

3) *Zero-inflated Poisson process*: A zero-inflated Poisson process  $\Phi$  (from [28]) is characterized by a parameter  $0 \leq p \leq 1$ , a rate  $\lambda \geq 0$ , and a spatial distribution  $s$ . It describes a population that is 1) either empty, or 2) non-empty, with size following a Poisson distribution and whose individual states are i.i.d. according to  $s$ . Its projection measures are given by

$$P_{\Phi}^{(n)}(B_1 \times \dots \times B_n) = \begin{cases} 1 - p + pe^{-\lambda}, & n = 0, \\ pe^{-\lambda} \frac{\lambda^n}{n!} \prod_{i=1}^n s(B_i), & \text{otherwise.} \end{cases} \quad (27)$$

Note that a Poisson process is a special case of a zero-inflated Poisson process in which the parameter  $p$  is set to one.

**Proposition 7** (p.g.fl. of a zero-inflated Poisson process). *The p.g.fl. of a zero-inflated Poisson process  $\Phi$  with parameter  $p$ , rate  $\lambda$ , and spatial distribution  $s$  is given by*

$$G_{\Phi}(h) = 1 - p + p \exp \left[ \lambda \left( \int h(x)s(dx) - 1 \right) \right]. \quad (28)$$

4) *I.i.d. process*: An i.i.d. process  $\Phi$  is characterized by a cardinality distribution  $\rho$  and a spatial distribution  $s$ . It describes a population whose size is distributed according to  $\rho$ , and whose individual states are i.i.d. according to  $s$ . Its Janossy measures are given by

$$J_{\Phi}^{(n)}(B_1 \times \dots \times B_n) = n! \rho(n) \prod_{i=1}^n s(B_i). \quad (29)$$

Note that a Poisson process is a special case of i.i.d. process in which the cardinality distribution  $\rho$  is Poisson.

### C. Prediction step

In this section, we propose an alternative expression of the original CPHD time prediction step [6] in which newborn targets originate from a spawning mechanism rather than spontaneous birth. Note that the assumptions on the posterior multi-target process from the previous time step, the target survival mechanism, and the target evolution mechanism are identical to the original assumptions in [6].

**Theorem 1** (CPHD with spawning: prediction step). *Assuming that, at step  $k$ :*

- *The posterior multi-target process  $\Phi_{k-1}$  is an i.i.d. process with intensity measure  $\mu_{k-1}$ , with cardinality distribution  $\rho_{k-1}$ , and spatial distribution  $s_{k-1}$ ,*
- *A target in state  $x$  at time  $k-1$  survived to time  $k$  with probability  $p_{s,k}(x)$ ,*
- *A surviving target in state  $x$  at time  $k-1$  evolved since time  $k-1$  according to a Markov transition  $f_{s,k}(\cdot|x)$ ,*
- *There was no spontaneous target birth since time  $k-1$ ,*
- *Newborn targets were spawned from prior targets (see next page),*

*then the intensity measure  $\mu_{k|k-1}$  and cardinality distribution  $\rho_{k|k-1}$  of the predicted multi-target process  $\Phi_{k|k-1}$  are given by*

$$\mu_{k|k-1}(\cdot) = \int [p_{s,k}(x)f_{s,k}(\cdot|x) + \mu_{b,k}(\cdot|x)] \mu_{k-1}(dx), \quad (30)$$

$$\rho_{k|k-1}(n) = \sum_{j=1}^n B_{n,j}(b_1, \dots, b_n) \times \left[ \sum_{m \geq j} \frac{m!}{n!(m-j)!} \rho_{k-1}(m) b_0^{m-j} \right], \quad (31)$$

where  $B_{n,j}$  is the partial Bell polynomial [29] given by

$$B_{n,k}(x_1, x_2, \dots, x_n) = \sum_{\substack{k_1+2k_2+\dots+nk_n=n \\ k_1+k_2+\dots+k_n=k}} \frac{n!}{k_1!(1!)^{k_1} k_2!(2!)^{k_2} \dots k_n!(n!)^{k_n}} x_1^{k_1} x_2^{k_2} \dots x_n^{k_n}, \quad (32)$$

and where the intensity measure  $\mu_{b,k}$  and the coefficients  $b_i$  are the parameters of the spawning process, dependent on the modeling choices. Denoting  $\bar{p}_{s,k}(\cdot) \equiv 1 - p_{s,k}(\cdot)$  and  $\bar{p}_{b,k}(\cdot) \equiv 1 - p_{b,k}(\cdot)$ , the parameters are as follows:

a) *Bernoulli process, with parameter  $p_{b,k}$  and spatial distribution  $s_{b,k}$ :*

$$\mu_{b,k}(\cdot|x) = p_{b,k}(x) s_{b,k}(\cdot|x), \quad (33)$$

and

$$b_i = \begin{cases} \int \bar{p}_{s,k}(x) \bar{p}_{b,k}(x) s_{k-1}(dx), & i = 0, \\ \int [p_{s,k}(x) \bar{p}_{b,k}(x) + \bar{p}_{s,k}(x) p_{b,k}(x)] s_{k-1}(dx), & i = 1, \\ 2 \int p_{s,k}(x) p_{b,k}(x) s_{k-1}(dx), & i = 2, \\ 0, & i > 2. \end{cases} \quad (34)$$

b) *Poisson process, with rate  $\lambda_{b,k}$  and spatial distribution  $s_{b,k}$ :*

$$\mu_{b,k}(\cdot|x) = \lambda_{b,k}(x) s_{b,k}(\cdot|x), \quad (35)$$

and,

$$b_i = \int \lambda_{b,k}^{i-1}(x) e^{-\lambda_{b,k}(x)} \times [\bar{p}_{s,k}(x) \lambda_{b,k}(x) + i p_{s,k}(x)] s_{k-1}(dx) \quad i \geq 0, \quad (36)$$

c) *zero-inflated Poisson process, with parameter  $p_{b,k}$ , rate  $\lambda_{b,k}$ , and spatial distribution  $s_{b,k}$ :*

$$\mu_{b,k}(\cdot|x) = p_{b,k}(x) \lambda_{b,k}(x) s_{b,k}(\cdot|x), \quad (37)$$

and,

$$b_i = \begin{cases} \int \bar{p}_{s,k}(x) [\bar{p}_{b,k}(x) + p_{b,k}(x) e^{-\lambda_{b,k}(x)}] s_{k-1}(dx), & i = 0, \\ \int [\bar{p}_{s,k} + p_{s,k}(x) [\bar{p}_{b,k}(x) + p_{b,k}(x) e^{-\lambda_{b,k}(x)}]] s_{k-1}(dx), & i = 1, \\ \int p_{b,k}(x) \lambda_{b,k}^{i-1}(x) e^{-\lambda_{b,k}(x)} \times [\bar{p}_{s,k}(x) \lambda_{b,k}(x) + i p_{s,k}(x)] s_{k-1}(dx), & i \geq 2. \end{cases} \quad (38)$$

The proof is given in the Appendix. Note that the structure of the predicted cardinality (31) allows for its efficient computation through an algorithm dedicated to the computation of partial Bell polynomials (see [29], [30] for examples).

#### IV. SIMULATION

In this section we illustrate the CPHD filter with spawning models through a simulation-based scenario. The Gaussian Mixture (GM) implementation of the CPHD filter is briefly described in Section IV-A, followed by a description of the metrics exploited for the analysis of the filter results in Section IV-B. The scenario and the selection of the filter parameters are detailed in Section IV-C, and the results are discussed in Section IV-D.

##### A. The GM-CPHD filter with spawning

Since the incorporation of spawning in the CPHD filtering process does not affect the data update step, we shall focus in this section on the specifics of the prediction step for the GM-CPHD filter with spawning. A description of the usual GM-CPHD, including the implementation of the spontaneous birth term, is given in [27].

1) *Filtering assumptions:* We follow the usual assumptions of the GM-CPHD filter [27] regarding the transition process from time  $k-1$  to time  $k$ , namely, that the probability of survival  $p_{s,k}$  is uniform over the state space  $\mathbf{X}$  and the transition  $f_{s,k}$  follows a linear Gaussian dynamical model:

$$p_{s,k}(\cdot) \equiv p_{s,k}, \quad (39)$$

$$f_{s,k|k-1}(\cdot|x) = \mathcal{N}(\cdot; F_k x, Q_k), \quad (40)$$

where  $\mathcal{N}(\cdot; m, P)$  denotes a Gaussian distribution with mean  $m$  and covariance  $P$ ,  $F_k$  is a state transition matrix, and  $Q_k$  is a process noise covariance matrix.

Regardless of the chosen spawning model (see Theorem 1), we further assume that the spatial distribution of each spawned object  $s_{b,k}$  can be described as the Gaussian mixture

$$s_{b,k}(\cdot|x) = \sum_{j=1}^{J_{b,k}} w_{b,k}^{(j)} \mathcal{N}(\cdot; F_{b,k}^{(j)} x + d_{b,k}^{(j)}, Q_{b,k}^{(j)}), \quad (41)$$

where  $d_{b,k}^{(j)}$  is a deviation vector,  $F_{b,k}^{(j)}$  is a spawning transition matrix, and  $Q_{b,k}^{(j)}$  is a spawning noise covariance matrix, for  $1 \leq j \leq J_{b,k}$ , and  $\sum_{j=1}^{J_{b,k}} w_{b,k}^{(j)} = 1$ . Also, we assume that the model parameters  $p_{b,k}$ ,  $\lambda_{b,k}$ , when applicable, are uniform over the state space  $\mathbf{X}$ :

$$p_{b,k}(\cdot) \equiv p_{b,k}, \quad (42)$$

$$\lambda_{b,k}(\cdot) \equiv \lambda_{b,k}.$$

2) *Predicted intensity:* The construction of the predicted intensity  $\mu_{k|k-1}$  in Eq. (30) follows a similar structure as for the usual GM-CPHD filter [31]. Assume that the posterior intensity  $\mu_{k-1}$  can be written as a Gaussian mixture of the form

$$\mu_{k-1}(\cdot) = \sum_{j=1}^{J_{k-1}} w_{k-1}^{(j)} \mathcal{N}(\cdot; m_{k-1}^{(j)}, P_{k-1}^{(j)}), \quad (43)$$

where  $m_{k-1}^{(j)}$  (resp.  $P_{k-1}^{(j)}$ ) is the posterior mean (resp. covariance) of the  $j$ -th component of the mixture. Then the predicted intensity  $\mu_{k|k-1}$  can also be written as a Gaussian mixture of the form

$$\mu_{k|k-1}(\cdot) = \mu_{s,k|k-1}(\cdot) + \mu_{b,k|k-1}(\cdot), \quad (44)$$

where the surviving component  $\mu_{s,k|k-1}$  is the Gaussian mixture

$$\mu_{s,k|k-1}(\cdot) = p_{s,k} \sum_{j=1}^{J_{k-1}} w_{k-1}^{(j)} \mathcal{N}(\cdot; m_{s,k|k-1}^{(j)}, P_{s,k|k-1}^{(j)}), \quad (45)$$

with

$$m_{s,k|k-1}^{(j)} = F_k m_{k-1}^{(j)}, \quad (46)$$

$$P_{s,k|k-1}^{(j)} = Q_k + F_k P_{k-1}^{(j)} F_k^T, \quad (47)$$

for  $1 \leq j \leq J_{k-1}$ , and the spawning component  $\mu_{b,k|k-1}$  is the Gaussian mixture

$$\begin{aligned} \mu_{b,k|k-1}(\cdot) &= \alpha_{b,k} \sum_{j=1}^{J_{k-1}} w_{k-1}^{(j)} \sum_{i=1}^{J_{b,k}} w_{b,k}^{(i)} \mathcal{N}(\cdot; m_{b,k|k-1}^{(j,i)}, P_{b,k|k-1}^{(j,i)}), \end{aligned} \quad (48)$$

with

$$m_{b,k|k-1}^{(j,i)} = F_{b,k}^{(i)} m_{k-1}^{(j)} + d_{b,k}^{(i)}, \quad (49)$$

$$P_{b,k|k-1}^{(j,i)} = Q_{b,k}^{(i)} + F_{b,k}^{(i)} P_{k-1}^{(j)} (F_{b,k}^{(i)})^T, \quad (50)$$

for  $1 \leq j \leq J_{k-1}$ ,  $1 \leq i \leq J_{b,k}$ , and the scalar  $\alpha_{b,k}$  depends on the spawning model:

$$\alpha_{b,k} = \begin{cases} p_{b,k}, & \text{Bernoulli process,} \\ \lambda_{b,k}, & \text{Poisson process,} \\ p_{b,k} \lambda_{b,k}, & \text{zero-inflated Poisson process.} \end{cases} \quad (51)$$

3) *Predicted cardinality distribution*: Due to the assumptions presented in Section IV-A1, the coefficients of the Bell polynomial in Eq. (31) have the simpler form

a) Bernoulli process:

$$b_i = \begin{cases} (1 - p_{s,k})(1 - p_{b,k}), & i = 0, \\ p_{s,k}(1 - p_{b,k}) + (1 - p_{s,k})p_{b,k}, & i = 1, \\ 2p_{s,k}p_{b,k}, & i = 2, \\ 0, & i > 2. \end{cases} \quad (52)$$

b) Poisson process:

$$b_i = \lambda_{b,k}^{i-1} e^{-\lambda_{b,k}} [(1 - p_{s,k}) \lambda_{b,k} + i p_{s,k}], \quad i \geq 0. \quad (53)$$

c) zero-inflated Poisson process:

$$b_i = \begin{cases} (1 - p_{s,k})(1 - p_{b,k} + p_{b,k} e^{-\lambda_{b,k}}), & i = 0, \\ (1 - p_{s,k}) p_{b,k} e^{-\lambda_{b,k}} \lambda_{b,k}, & i = 1, \\ p_{b,k} \lambda_{b,k}^{i-1} e^{-\lambda_{b,k}} [(1 - p_{s,k}) \lambda_{b,k} + i p_{s,k}], & i \geq 2. \end{cases} \quad (54)$$

The predicted cardinality distribution is then computed by the appropriate substitution of Eqs. (52)-(54) into Eq. (31).

## B. Evaluation metrics

To compare the multi-target state representing the true targets in the scene – the “ground truth” – and a collection of targets extracted from the filter’s output, we exploit the Optimal Sub-Pattern Assignment (OSPA) metric [32] for assessing the accuracy of multi-object filters. Given two sets  $X = \{x_1, \dots, x_m\}$ ,  $x_i \in \mathbf{X}$ ,  $1 \leq i \leq m$ , and  $Y = \{y_1, \dots, y_n\}$ ,  $y_j \in \mathbf{X}$ ,  $1 \leq j \leq n$ , the second-order OSPA distance  $d_2^{(c)}(X, Y)$  between  $X$  and  $Y$  is defined as

$$d_2^{(c)}(X, Y) = \begin{cases} 0, & m = n = 0, \\ \left[ \frac{1}{n} \left( \min_{\pi \in \Pi_n} \sum_{i=1}^m d^{(c)}(x_i, y_{\pi(i)})^2 + c^2(n - m) \right) \right]^{1/2}, & m \leq n, \\ d_2^{(c)}(Y, X), & \text{otherwise,} \end{cases} \quad (55)$$

with

$$d^{(c)}(x_i, y_j) = \min(c, \|x_i - y_j\|), \quad (56)$$

where  $c$  is the cutoff parameter, and  $\|\cdot\|$  is the usual norm on  $\mathbf{X}$ . The OSPA distance is such that  $0 \leq d_2^{(c)}(X, Y) \leq c$ ;  $d_2^{(c)}(X, Y) = 0$  indicates that  $X$  and  $Y$  are identical, while  $d_2^{(c)}(X, Y)$  increases with the discrepancies between  $X$  and  $Y$ , taking into account mismatches in number of elements and element states.

In order to compare the true number of targets in the scene and a estimated cardinality distribution extracted from the filter’s output, we exploit the Hellinger distance [33]. Given two finite cardinality distributions  $P = (p_1, \dots, p_k)$  and  $Q = (q_1, \dots, q_k)$ , the Hellinger distance  $d_H(P, Q)$  is

$$d_H(P, Q) = \frac{1}{\sqrt{2}} \sqrt{\sum_{i=1}^k (\sqrt{p_i} - \sqrt{q_i})^2}. \quad (57)$$

Note that in (57), the coefficient  $1/\sqrt{2}$  is included in order to scale the Hellinger distance such that it is bounded as  $0 \leq d_H(P, Q) \leq 1$ ;  $d_H(P, Q) = 0$  indicates that  $P$  and  $Q$  are equivalent, where as  $d_H(P, Q) \rightarrow 1$ ,  $P$  and  $Q$  become increasingly dissimilar.

## C. Scenario and filter setup

A point  $[x, y, \dot{x}, \dot{y}]$  of the single-target state space  $\mathbf{X} \subset \mathbb{R}^4$  describes the position and velocity coordinates of an object in a square surveillance region of size  $2000 \text{ m} \times 2000 \text{ m}$ . The simulated multi-target tracking scenario consists of one scan per second for 100 s, and up to seven targets evolving in the region with constant velocity. Two targets are present at the beginning of the scenario and each spawns targets at different times: target 1 spawns two additional targets at  $t = 15 \text{ s}$  and target 2 spawns three additional targets at  $t = 25 \text{ s}$ . All spawned targets have a lifespan of 60 s. Fig. 1 shows the trajectories of the targets cumulated over time, while Fig. 2 illustrates these trajectories and the collected measurements

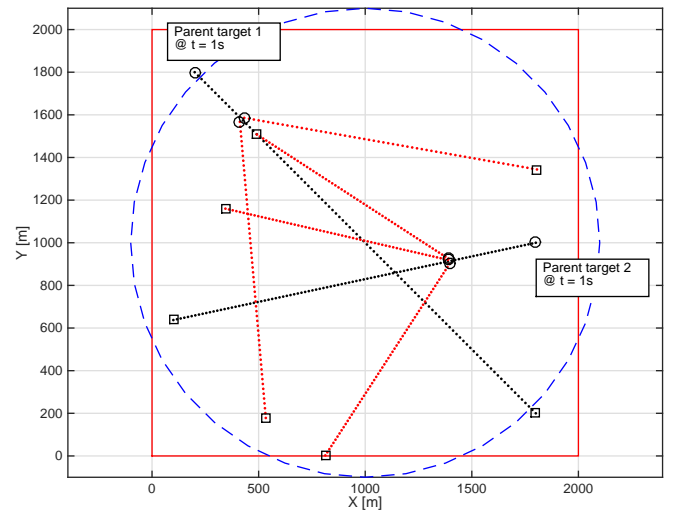


Fig. 1: Target trajectories. A circle “○” indicates where a trajectory begins, and a square “□” indicates where a trajectory ends. The large square indicates the limits of the sensor’s FoV and the large dashed circle represents the 90% confidence region of the Gaussian component of the spontaneous birth model.

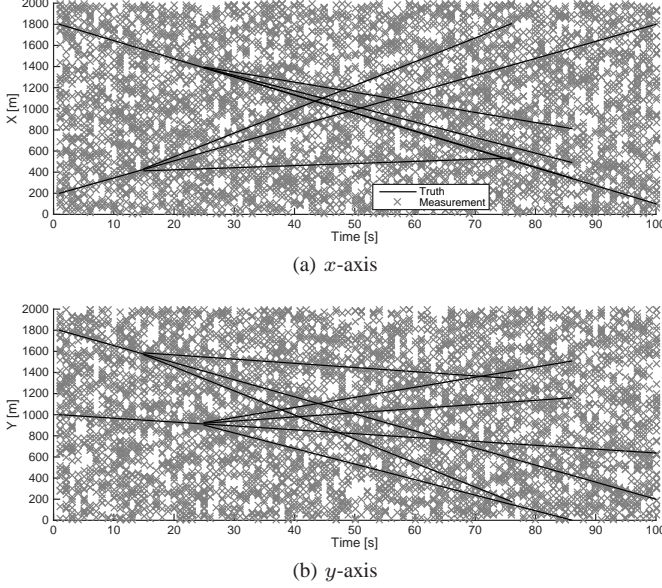


Fig. 2: Collected measurements (gray crosses) and target positions (black lines).

The probability of survival  $p_{s,k}$  (39) is constant throughout the scenario, and set to  $p_{s,k} = 0.99$ . The target motion model  $f_{s,k|k-1}$  (40) is set as follows:

$$F_k = \begin{bmatrix} \mathbf{1}_2 & \Delta \mathbf{1}_2 \\ \mathbf{0}_2 & \mathbf{1}_2 \end{bmatrix}, \quad Q_k = \sigma_\nu^2 \begin{bmatrix} \frac{\Delta^4}{4} \mathbf{1}_2 & \frac{\Delta^3}{2} \mathbf{1}_2 \\ \frac{\Delta^3}{2} \mathbf{1}_2 & \Delta^2 \mathbf{1}_2 \end{bmatrix}, \quad (58)$$

where  $\Delta = 1$  s,  $\sigma_\nu = 5$  m s<sup>-2</sup>, and  $\mathbf{1}_n$  (resp.  $\mathbf{0}_n$ ) denotes the  $n \times n$  identity (resp. zero) matrix.

The sensor's probability of detection is uniform over the sensor's FoV, and set at a constant value of 0.95 throughout the scenario. Each target-generated measurement consists of the target's coordinate position with an independent Gaussian white noise on each component, with a standard deviation of 10 m. Spurious measurements are modeled as a Poisson point process with uniform spatial distribution over the state space and an average number of clutter per unit volume of  $12.5 \times 10^{-6}$  m<sup>-2</sup>, that is, an average of 50 clutter returns per scan over the surveillance region.

For the sake of comparison, the usual GM-CPHD [27] with spontaneous birth and no spawning is implemented as well. The spontaneous birth model is Poisson, with constant rate of 0.025 per time step (which yields, over 100 s of the scenario, an average of 2.5 newborn targets each parent target). The spatial distribution is modeled with single Gaussian component, centered on the sensor's FoV illustrated in Fig. 1.

The spatial distribution of the spawning (41) is identical for the three considered models. We assume no spawned target deviation vectors, and a standard deviation of 12 units is set on each component of the spawning noise covariance, i.e.

$$F_{b,k} = \begin{bmatrix} \mathbf{1}_2 & \mathbf{0}_2 \\ \mathbf{0}_2 & \mathbf{1}_2 \end{bmatrix}, \quad d_{b,k} = \mathbf{0}, \quad Q_{b,k} = \begin{bmatrix} \sigma_b^2 \mathbf{1}_2 & \mathbf{0}_2 \\ \mathbf{0}_2 & \dot{\sigma}_b^2 \mathbf{1}_2 \end{bmatrix}, \quad (59)$$

where  $\mathbf{0}$  denotes the null vector in  $\mathbf{X}$ ,  $\sigma_b = 12$  m, and  $\dot{\sigma}_b = 12$  m s<sup>-1</sup>.

The parameters of the three spawning models are set as follows. The zero-inflated Poisson model assumes one spawning per parent target during the scenario with an average of 2.5 daughter targets per spawning event, thus  $p_{b,k}$  and  $\lambda_b$  are set to 0.01 and 2.5, respectively. Relative to the zero-inflated Poisson model, the Poisson model is set to yield a similar spawning intensity thus its  $\lambda_{b,k}$  is set to 0.025, whereas the Bernoulli model is set to yield a similar spawning frequency so its  $p_{b,k}$  is set to 0.01. These parameters are also presented in Table I.

TABLE I: Spawn model parameters.

Model	$p_{b,k}$	$\lambda_{b,k}$	$\mu_{b,k}(\cdot x)$
Bernoulli	0.01	-	$0.01\mathcal{N}(\cdot; x, Q_{b,k})$
Poisson	-	0.025	$0.025\mathcal{N}(\cdot; x, Q_{b,k})$
zero-inflated Poisson	0.01	2.5	$0.025\mathcal{N}(\cdot; x, Q_{b,k})$

It is interesting to note that neither the Poisson nor the Bernoulli models are equipped to capture the nature of the spawning events occurring in this scenario, since, per construction, the Poisson model is a poor match for spawning events occurring at unknown dates and the Bernoulli model is a poor match for spawning events creating more than one daughter target. The zero-inflated Poisson model possesses a greater flexibility and should be able to cope with a wider range of spawning situations; in any case, it is expected to yield better performances on the scenario presented in this paper.

To maintain tractability, GM components are truncated with threshold  $T = 10^{-5}$ , pruned with maximum number of components  $J_{\max} = 100$ , and merged with threshold  $U = 4$  (see [31] for more details on the pruning and merging mechanisms). Additionally, the maximum number of targets is set to  $N_{\max} = 20$  to circumvent issues with infinitely tailed cardinality distributions [27].

#### D. Simulation results

The proposed spawning models and the birth model are implemented with the GM-CPHD filter, and compared over 500 Monte Carlo (MC) runs of the multi-target scenario described in Section IV-C.

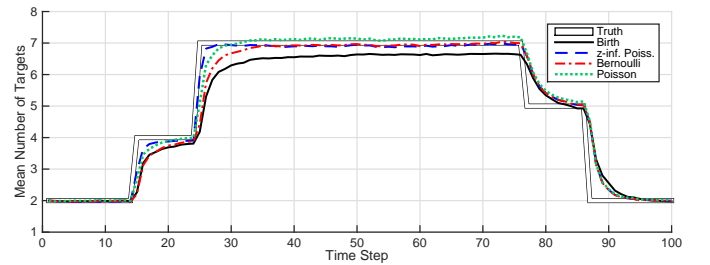


Fig. 3: MAP estimate of the number of targets (averaged on 500 runs).

The MAP estimate of the number of targets is plotted in Fig. 3, along with the true number of targets in the scene. The results suggest that the spawning models provide a better estimate of the number of targets and, in particular, converge faster to the true number of targets following the appearance of new targets in the scene. This is expected, because the



scenario does not feature any spontaneous but only spawning related births, and thus in this context spawning models are a better match than the birth model.

Among the three spawning models, the zero-inflated Poisson converges the fastest following the appearance of new targets while the Bernoulli model converges the slowest. This is expected, for the zero-inflated Poisson model provides the best match to the spawning events occurring in this scenario. Note in particular that the Bernoulli model may not consider the appearance of more than one daughter per spawning event, and must therefore stage the multiple-target appearance across several successive time steps; in other words, the Bernoulli is ill-adapted to “busy” events where targets appear simultaneously. Note also the slight overestimation shown by the Poisson model when the true number of target is stable. Per construction, the Poisson model is well-equipped for the simultaneous appearance of an arbitrary number of spawned targets at any time step, but it fails at coping with “quiet” periods where no spawning occurs because, unlike the zero-inflated Poisson model, it does not temper the Poisson-driven spawning with a probability of spawning. In other words, the Poisson model is ill-adapted to the spawning events shown in this scenario.

Note that all models – spawning and birth – follow the same mechanism for target deaths and yield much closer performances when target disappearances occur.

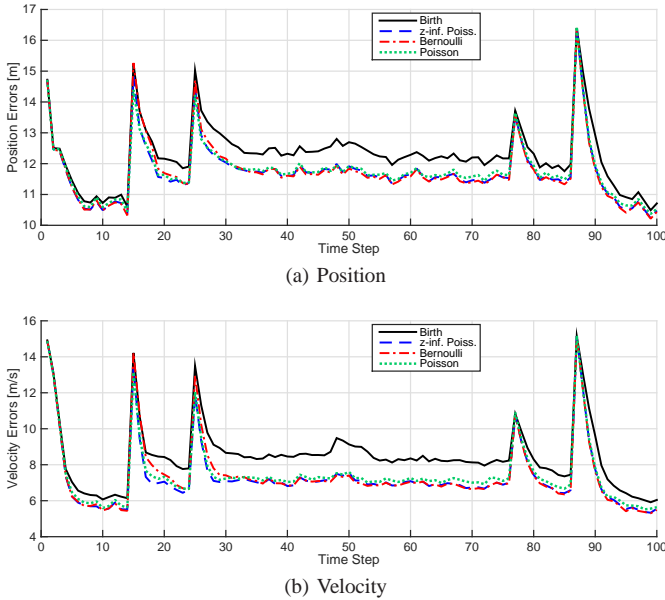


Fig. 4: OSPA distance (averaged on 500 runs).

Similar conclusions can be drawn from the comparisons of the OSPA distances shown in Fig. 4. All models show error spikes at times of spawning ( $t = 15$  s,  $t = 25$  s) and death ( $t = 76$  s,  $t = 86$  s), however, the spawning models recover more quickly than the birth model, and have consistently lower errors.

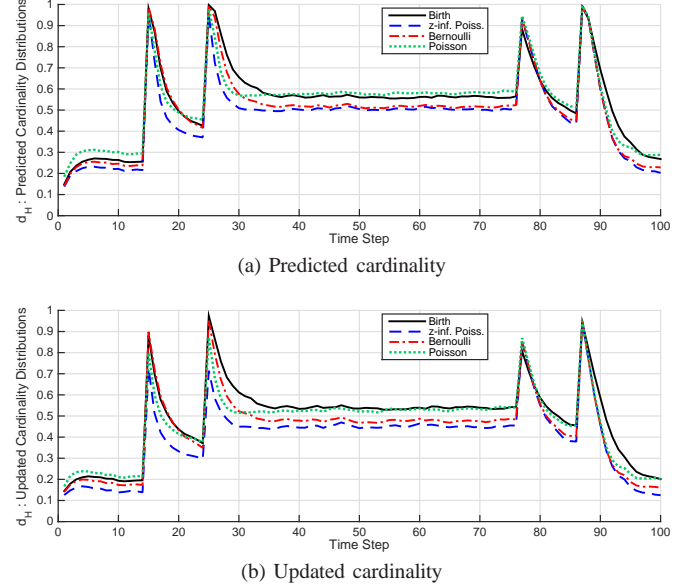


Fig. 5: Hellinger distances (averaged on 500 runs).

The quality of the estimation of the number of targets proposed by the four models is further illustrated in Fig. 5, where the Hellinger distance between the cardinality distribution propagated by each model and the “ideal” cardinality distribution (i.e., a distribution in which all the mass is concentrated on the true number of targets).

The results in Fig. 5 allow a more refined analysis of the proposed models. All the models yield poor estimates immediately after a change in the true number of targets<sup>5</sup>, but the zero-inflated Poisson model converges the fastest following a target birth/death and it converges to the best estimate during periods where the number of target is stable. The Poisson model converges *faster* than the Bernoulli model, but to a *worse* estimate: this is expected, since the Poisson model is ill-adapted to “quiet” periods while the Bernoulli model is ill-adapted to “busy” events (see discussion above on Fig. 3).

As expected, the updated cardinality distributions are consistently more accurate than the predicted cardinality distributions since they benefit from the processing of an additional measurement batch.

## V. CONCLUSION

The motivation for the work presented in this paper is the resolution of multi-object detection and tracking problems in which newborn objects are spawned from preexisting ones. To this end, the construction of a CPHD filter in which the appearance of newborn targets is modeled with a spawning mechanism rather than spontaneous birth is proposed, based on a principled derivation procedure within the FISST framework.

A GM implementation of the CPHD filter with spawning is then presented, considering three different models for the spawning mechanism based on a Bernoulli, a Poisson, or a zero-inflated Poisson process. The three resulting filters are

<sup>5</sup>Recall from Eq. (57) that the Hellinger distance  $d_H$  is such that  $0 \leq d_H \leq 1$ .

then illustrated, analyzed, and compared to a usual CPHD filter with spontaneous birth but no spawning, on the same simulated scenario involving two parent targets spawning a total of five daughter targets. Results show that a spawning model, appropriately chosen for a given application, can provide better estimates than a spontaneous birth model.

#### ACKNOWLEDGEMENT

Daniel Bryant's work is supported by the Science, Mathematics & Research for Transformation (SMART) Scholarship-for-Service Program.

Emmanuel Delande and Daniel Clark are supported by the Engineering and Physical Sciences Research Council (EPSRC) Platform Grant (EP/J015180/1), the MOD University Defence Research Centre on Signal Processing (UDRC) Phase 2 (EP/K014227/1).

Daniel Clark wishes to thank Professor Penina Axelrad in the Aerospace Department in Boulder for supporting his Visiting Professor position through the Faculty-in-Residence Summer Term (FIRST) programme at the University of Colorado Boulder in summer 2014.

The authors would also like to thank Nicola Baresi and In-Kwan Park of the University of Colorado at Boulder and Illán Amor of Universidad de Oviedo, Asturias Spain for their conversations and ideas early on for this work during the FIRST programme.

#### APPENDIX

##### A. Proof of theorem 1

For the sake of simplicity, the time subscripts will be omitted throughout the proof when there is no ambiguity. Also, we will denote by  $\bar{p}_s$  (resp.  $\bar{p}_d$ ) the function  $1 - p_{s,k}$  (resp.  $1 - p_{d,k}$ ).

1) *Predicted p.g.fl.*: Let us focus first on the p.g.fl.  $G_{k|k-1}$  of the predicted multi-target point process  $\Phi_{k|k-1}$ . Each parent target in the population, represented by the prior point process  $\Phi_{k-1}$ , generates daughter targets in the predicted population in two ways:

- a daughter target stemming from the (eventual) survival of the parent target, represented by a survival point process  $\Phi_s$ ,
- a population of daughter spawned from the parent target, represented by a spawning point process  $\Phi_b$ .

Using Eq. (8), and denoting by  $G_s$  (resp.  $G_b$ ) the p.g.fl. of the survival (resp. spawning) point process, we can describe the evolution of a parent target with state  $x \in \mathbf{X}$  with a compound process with p.g.fl.

$$G_c(h|x) = G_s(h|x)G_b(h|x), \quad (60)$$

and exploiting the Galton-Watson equation (9), we may finally write

$$G_{k|k-1}(h) = G_{k-1}(G_c(h|\cdot)) \quad (61a)$$

$$= G_{k-1}(G_s(h|\cdot)G_b(h|\cdot)). \quad (61b)$$

2) *Predicted intensity*: Let us now focus on the expression of the predicted intensity  $\mu_{k|k-1}$ . For that, let us fix an arbitrary measurable subset  $B \in \mathbf{B}_\mathbf{X}$ . The expression of the intensity evaluated in  $B$  can be recovered from the first derivative of the p.g.fl.  $G_{k|k-1}$  using Eq. (20):

$$\mu_{k|k-1}(B) = \delta G_{k|k-1}(h; 1_B) \Big|_{h=1} \quad (62a)$$

$$= \delta(G_{k-1}(G_c(h|\cdot)); 1_B) \Big|_{h=1} \quad (62b)$$

Using the definition of the p.g.fl. (5a) then yields

$$\mu_{k|k-1}(B) = \delta \left( \int_{\mathcal{X}} \left[ \prod_{x \in \varphi} G_c(h|x) \right] P_{k-1}(d\varphi; 1_B) \right) \Big|_{h=1} \quad (62c)$$

$$= \int_{\mathcal{X}} \delta \left( \prod_{x \in \varphi} G_c(h|x); 1_B \right) \Big|_{h=1} P_{k-1}(d\varphi) \quad (62d)$$

From the product rule (14) it follows that

$$\begin{aligned} \mu_{k|k-1}(B) = & \int_{\mathcal{X}} \sum_{x \in \varphi} \left[ \delta G_c(h|x; 1_B) \Big|_{h=1} \prod_{\substack{\bar{x} \in \varphi \\ \bar{x} \neq x}} \underbrace{G_c(1|\bar{x})}_{=1} \right] P_{k-1}(d\varphi) \\ & (62e) \end{aligned}$$

Using the product rule (14) on  $G_c(\cdot|x) = G_s(\cdot|x)G_b(\cdot|x)$  then yields

$$\begin{aligned} \mu_{k|k-1}(B) &= \int_{\mathcal{X}} \sum_{x \in \varphi} \left[ \delta G_s(h|x; 1_B) \Big|_{h=1} \underbrace{G_b(1|x)}_{=1} \right. \\ &\quad \left. + \underbrace{G_s(1|x)}_{=1} \delta G_b(h|x; 1_B) \Big|_{h=1} \right] P_{k-1}(d\varphi) \end{aligned} \quad (62f)$$

Using Eq. (20) we introduce the intensity  $\mu_s$  (resp.  $\mu_b$ ) of the survival (resp. spawning) process and we obtain:

$$\mu_{k|k-1}(B) = \int_{\mathcal{X}} \sum_{x \in \varphi} [\mu_s(B|x) + \mu_b(B|x)] P_{k-1}(d\varphi) \quad (62g)$$

Which becomes, using Campbell's theorem [34, p. 271]:

$$\mu_{k|k-1}(B) = \int [\mu_s(B|x) + \mu_b(B|x)] \mu_{k-1}(dx). \quad (62h)$$

Note that the validity of the expression of the predicted intensity above is not restricted to specific models for the prior process  $\Phi_{k-1}$ . As such, the construction of the predicted intensity is identical in the case of the PHD filter with spawning (see Mahler's original proof in [5]). Let us now focus on the explicit expression of the intensity measure  $\mu_s$ . Since the survival process is assumed Bernoulli with parameter  $p_s(\cdot)$  and spatial distribution  $f_s(\cdot|.)$ , we can exploit Eq. (20) to retrieve the intensity  $\mu_s$  through the expression of the p.g.fl.  $G_s$  given by Eq. (24):

$$\mu_s(B|.) = \delta G_s(h|.; 1_B) \Big|_{h=1} \quad (63a)$$

$$= \delta \left( 1 - p_s(\cdot) + p_s(\cdot) \int h(x) f_s(dx|.) ; 1_B \right) \Big|_{h=1} \quad (63b)$$

$$= p_s(\cdot) f_s(B|.). \quad (63c)$$

Let us now focus on the explicit expression of the intensity measure  $\mu_b$  of the spawning process, depending on the modeling choices.

a) Bernoulli process with parameter  $p_b(\cdot)$  and spatial distribution  $s_b(\cdot|.)$ :

Using the same construction as in Eq. (63) we have immediately

$$\mu_b(B|.) = p_b(\cdot) s_b(B|.). \quad (64)$$

b) zero-inflated Poisson process with parameter  $p_b(\cdot)$ , rate  $\lambda_b(\cdot)$  and spatial distribution  $s_b(\cdot|.)$ :

Exploiting Eq. (28) yields

$$\begin{aligned} \mu_b(B|.) &= \delta G_b(h|.; 1_B) \Big|_{h=1} \end{aligned} \quad (65a)$$

$$= \delta \left( \bar{p}_b(\cdot) + p_b(\cdot) \exp \left[ \lambda_b(\cdot) \left( \int h(x) s_b(dx|.) - 1 \right) \right] ; 1_B \right) \Big|_{h=1} \quad (65b)$$

$$\begin{aligned} &= p_b(\cdot) \lambda_b(\cdot) \delta \left( \int h(x) s_b(dx|.) - 1 ; 1_B \right) \Big|_{h=1} \\ &\quad \times \underbrace{\exp \left[ \lambda_b(\cdot) \left( \int s_b(dx|.) - 1 \right) \right]}_{=0} \end{aligned} \quad (65c)$$

$$= p_b(\cdot) \lambda_b(\cdot) s_b(B|.). \quad (65d)$$

3) *Predicted cardinality*: Let us now focus on the expression of the predicted cardinality  $\rho_{k|k-1}$ . From Eq. (4) the cardinality distribution of an arbitrary point process can be retrieved through its Janossy measures; let us then compute the predicted  $n^{th}$ -order Janossy measure  $J_{k|k-1}^{(n)}$  evaluated at the neighborhood of a collection of  $n$  arbitrary points  $y_1, \dots, y_n$ . Using Eq. (19) yields

$$\begin{aligned} J_{k|k-1}^{(n)}(d(y_1, \dots, y_n)) &= \delta^n G_{k|k-1}(h; 1_{dy_1}, \dots, 1_{dy_n}) \Big|_{h=0} \end{aligned} \quad (66a)$$

$$= \delta^n (G_{k-1}(G_c(h|.); 1_{dy_1}, \dots, 1_{dy_n})) \Big|_{h=0} \quad (66b)$$

Applying the general chain rule (12) then gives

$$\begin{aligned} J_{k|k-1}^{(n)}(d(y_1, \dots, y_n)) &= \sum_{\pi \in \Pi_n} \delta^{|\pi|} G_{k-1} \left( G_c(h|.); \left( \delta^{|\omega|} G_c(h|.; (1_{dy_i})_{i \in \omega}) \right)_{\omega \in \pi} \right) \Big|_{h=0}. \end{aligned} \quad (66c)$$

Developing the predicted p.g.fl.  $G_{k-1}$  through Janossy measures with Eq. (2) then gives

$$\begin{aligned} J_{k|k-1}^{(n)}(d(y_1, \dots, y_n)) &= \sum_{\pi \in \Pi_n} \sum_{m \geq |\pi|} \frac{1}{(m - |\pi|)!} \int_{\mathbf{X}^m} \prod_{i=1}^{|\pi|} \delta^{|\omega_i|} G_c(h|x_i; (1_{dy_j})_{j \in \omega_i}) \Big|_{h=0} \\ &\quad \times \prod_{i=|\pi|+1}^m G_c(0|x_i) J_{k-1}^{(m)}(d(x_1, \dots, x_m)). \end{aligned} \quad (67)$$

Since the prior process is assumed i.i.d., we can substitute the expression given by Eq. (29) to the prior Janossy densities  $J_{k-1}^{(m)}$  and obtain

$$\begin{aligned} J_{k|k-1}^{(n)}(d(y_1, \dots, y_n)) &= \sum_{\pi \in \Pi_n} \sum_{m \geq |\pi|} \frac{m!}{(m - |\pi|)!} \rho(m) C_\pi(d(y_1, \dots, y_n)), \end{aligned} \quad (68)$$

where

$$C_\pi(d(y_1, \dots, y_n)) = \int \dots \int \prod_{i=1}^{|\pi|} \delta^{|\omega_i|} G_c(h|x_i; (1_{dy_j})_{j \in \omega_i}) \Big|_{h=0} \times \prod_{i=|\pi|+1}^m G_c(0|x_i) \prod_{i=1}^m s(dx_i) \quad (69a)$$

$$= \left( \int G_c(0|x) s(dx) \right)^{m-|\pi|} \times \prod_{\omega \in \pi} \left( \int \delta^{|\omega|} G_c(h|x; (1_{dy_i})_{i \in \omega}) \Big|_{h=0} s(dx) \right) \quad (69b)$$

Recall from Eq. (60) that  $G_c(h|x) = G_s(h|x)G_b(h|x)$ ; using the product rule (14) on Eq. (69b) then yields

$$C_\pi(d(y_1, \dots, y_n)) = \left( \int G_s(0|x) G_b(0|x) s(dx) \right)^{m-|\pi|} \times \prod_{\omega \in \pi} \left( \int \sum_{\nu \subseteq \omega} \delta^{|\nu|} G_s(h|x; (1_{dy_i})_{i \in \nu}) \Big|_{h=0} \delta^{|\omega|-|\nu|} G_b(h|x; (1_{dy_i})_{i \in \omega \setminus \nu}) \Big|_{h=0} s(dx) \right). \quad (70)$$

Now, from the derivation shown in Eq. (63), we see that:

$$\delta^{|\nu|} G_s(h|x; (1_{dy_i})_{i \in \nu}) \Big|_{h=0} = \begin{cases} 1 - p_s(x), & \nu = \emptyset, \\ p_s(x) f_s(dy_i|x), & \nu = \{i\}, \\ 0, & |\nu| > 1. \end{cases} \quad (71)$$

Therefore, Eq. (70) simplifies as follows:

$$C_\pi(d(y_1, \dots, y_n)) = \left( \int \bar{p}_s(x) G_b(0|x) s(dx) \right)^{m-|\pi|} \times \prod_{\omega \in \pi} \left( \int \bar{p}_s(x) \delta^{|\omega|} G_b(h|x; (1_{dy_i})_{i \in \omega}) \Big|_{h=0} s(dx) + \int \sum_{1_{dy_i} \in \omega} p_s(x) f_s(dy_i|x) \times \delta^{|\omega|-1} G_b(h|x; (1_{dy_j})_{j \in \omega \setminus \{i\}}) \Big|_{h=0} s(dx) \right). \quad (72)$$

We shall now detail the expression of Eq. (72) depending on the modeling choices for the spawning process.

a) Bernoulli process with parameter  $p_s(\cdot)$  and spatial distribution  $f_s(\cdot|\cdot)$ :

We may draw similar results from the derivation shown in Eq. (71):

$$\delta^{|\nu|} G_b(h|x; (1_{dy_j})_{j \in \nu}) \Big|_{h=0} = \begin{cases} 1 - p_b(x), & \nu = \emptyset, \\ p_b(x) s_b(dy_j|x), & \nu = \{j\}, \\ 0, & |\nu| > 1. \end{cases} \quad (73)$$

Therefore, Eq. (72) simplifies as follows

$$C_\pi(d(y_1, \dots, y_n)) = \left( \int \bar{p}_s(x) \bar{p}_b(x) s(dx) \right)^{m-|\pi|} \times \prod_{\{i\} \in \pi} \left( \int \bar{p}_s(x) p_b(x) s_b(dy_i|x) s(dx) + \int \bar{p}_b(x) p_s(x) f_s(dy_i|x) s(dx) \right) \times \prod_{\{i,j\} \in \pi} \left( \int p_s(x) p_b(x) f_s(dy_i|x) s_b(dy_j|x) s(dx) + \int p_s(x) p_b(x) f_s(dy_j|x) s_b(dy_i|x) s(dx) \right) \times \prod_{\substack{\omega \in \pi \\ |\omega| > 2}} 0. \quad (74)$$

Substituting Eq. (74) to Eq. (68), we may finally retrieve the scalar  $\rho_{k|k-1}(n)$  through Eq. (4):

$$\rho_{k|k-1}(n) = \frac{1}{n!} \int_{\mathbf{X}^n} J_{k|k-1}^{(n)}(d(y_1, \dots, y_n)) \quad (75a)$$

$$= \sum_{\pi \in \Pi_n} \sum_{m \geq |\pi|} \frac{m!}{n!(m-|\pi|)!} \rho(m) b_0^{m-|\pi|} \prod_{\omega \in \pi} b_{|\omega|}, \quad (75b)$$

where the coefficients  $b_i$  are defined by

$$b_i = \begin{cases} \int \bar{p}_s(x) \bar{p}_b(x) s(dx), & i = 0, \\ \int [p_s(x) \bar{p}_b(x) + \bar{p}_s(x) p_b(x)] s(dx), & i = 1, \\ 2 \int p_s(x) p_b(x) s(dx), & i = 2, \\ 0, & i > 2. \end{cases} \quad (76)$$

Using the definition of the Bell polynomial (32) then yields the desired result.

b) zero-inflated Poisson process with parameter  $p_b(\cdot)$ , rate  $\lambda_b(\cdot)$ , and spatial distribution  $s_b(\cdot|\cdot)$ :

Applying the chain rule (12) to the p.g.fl. (28) yields

$$\delta^{|\nu|} G_b(h|x; (1_{dy_j})_{j \in \nu}) \Big|_{h=0} = \begin{cases} 1 - p_b(x) + p_b(x) e^{-\lambda_b(x)}, & \nu = \emptyset, \\ p_b(x) e^{-\lambda_b(x)} \lambda_b(x)^{|\nu|} \prod_{j \in \nu} s_b(dy_j|x), & |\nu| > 0. \end{cases} \quad (77)$$



Therefore, Eq. (72) simplifies as follows

$$\begin{aligned}
C_\pi(d(y_1, \dots, y_n)) = & \left( \int \bar{p}_s(x) [\bar{p}_b(x) + p_b(x)e^{-\lambda_b(x)}] s(dx) \right)^{m-|\pi|} \\
& \times \prod_{\{i\} \in \pi} \left( \int \bar{p}_s(x) p_b(x) e^{-\lambda_b(x)} \lambda_b(x) s_b(dy_i|x) s(dx) \right. \\
& \quad \left. + \int p_s(x) (\bar{p}_b(x) + p_b(x)e^{-\lambda_b(x)}) f_s(dy_i|x) s(dx) \right) \\
& \times \prod_{\substack{\omega \in \pi \\ |\omega| > 1}} \left( \int \bar{p}_s(x) p_b(x) e^{-\lambda_b(x)} \lambda_b(x)^{|\omega|} \left[ \prod_{i \in \omega} s_b(dy_i|x) \right] s(dx) \right. \\
& \quad \left. + \int p_s(x) p_b(x) e^{-\lambda_b(x)} \lambda_b(x)^{|\omega|-1} \right. \\
& \quad \left. \times \sum_{i \in \omega} f_s(dy_i|x) \left[ \prod_{\substack{j \in \omega \\ j \neq i}} s_b(dy_j|x) \right] s(dx) \right). \quad (78)
\end{aligned}$$

Substituting Eq. (78) to Eq. (68), we may finally retrieve the scalar  $\rho_{k|k-1}(n)$  through Eq. (4):

$$\begin{aligned}
\rho_{k|k-1}(n) &= \frac{1}{n!} \int_{\mathbf{X}^n} J_{k|k-1}^{(n)}(d(y_1, \dots, y_n)) \quad (79a) \\
&= \sum_{\pi \in \Pi_n} \sum_{m \geq |\pi|} \frac{m!}{n!(m-|\pi|)!} \rho(m) b_0^{m-|\pi|} \prod_{\omega \in \pi} b_{|\omega|} \quad (79b)
\end{aligned}$$

where the coefficients  $b_i$  are defined by

$$b_i = \begin{cases} \int \bar{p}_s(x) [\bar{p}_b(x) + p_b(x)e^{-\lambda_b(x)}] s(dx), & i = 0, \\ \int [\bar{p}_s(x) p_b(x) e^{-\lambda_b(x)} \lambda_b(x) + p_s(x) [\bar{p}_b(x) + p_b(x)e^{-\lambda_b(x)}]] s(dx), & i = 1, \\ \int p_b(x) \lambda_b^{i-1}(x) e^{-\lambda_b(x)} [\bar{p}_s(x) \lambda_b(x) + i p_s(x)] s(dx), & i \geq 2. \end{cases} \quad (80)$$

Using the definition of the Bell polynomial (32) then yields the desired result.

## REFERENCES

- [1] T. E. Fortmann, Y. Bar-Shalom, and M. Scheffe, "Sonar tracking of multiple targets using joint probabilistic data association," *Oceanic Engineering, IEEE Journal of*, vol. 8, no. 3, pp. 173–184, Jul 1983.
- [2] D. Reid, "An Algorithm for Tracking Multiple Targets," *Automatic Control, IEEE Transactions on*, vol. 24, no. 6, pp. 843–854, Dec. 1979.
- [3] R. P. S. Mahler, *Statistical Multisource-Multitarget Information Fusion*. Artech House, 2007.
- [4] —, *Advances in Statistical Multisource-Multitarget Information Fusion*. Artech House, 2014.
- [5] —, "Multitarget Bayes Filtering via First-Order Multitarget Moments," *Aerospace and Electronic Systems, IEEE Transactions on*, vol. 39, no. 4, pp. 1152–1178, Oct. 2003.
- [6] —, "PHD Filters of Higher Order in Target Number," *Aerospace and Electronic Systems, IEEE Transactions on*, vol. 43, no. 4, pp. 1523–1543, Oct. 2007.
- [7] M. Swartwout, "A brief history of rideshares (and attack of the CubeSats)," in *Aerospace Conference, 2011 IEEE*, mar 2011, pp. 1–15.
- [8] —, "A statistical survey of rideshares (and attack of the CubeSats, part deux)," in *Aerospace Conference, 2012 IEEE*, mar 2012, pp. 1–7.
- [9] L. Anselmo and C. Pardini, "Analysis of the consequences in low Earth orbit of the collision between Cosmos 2251 and Iridium 33," in *21st International Symposium Space Flight Dynamics*, vol. 294, 2009.
- [10] N. L. Johnson, E. Stansbery, J.-C. Liou, M. Horstman, C. Stokely, and D. Whitlock, "The characteristics and consequences of the break-up of the Fengyun-1C spacecraft," *Acta Astronautica*, vol. 63, no. 1, pp. 128–135, 2008.
- [11] B. A. Jones, D. S. Bryant, B.-T. Vo, and B.-N. Vo, "Challenges of Multi-Target Tracking for Space Situational Awareness," ser. Information Fusion, Proceedings of the 18th International Conference on, July 2015.
- [12] B. A. Jones, S. Gehly, and P. Axelrad, "Measurement-based Birth Model for a Space Object Cardinalized Probability Hypothesis Density Filter," *AIAA/AAS Astrodynamics Specialist Conference*, Aug. 2014.
- [13] M. Lundgren, L. Svensson, and L. Hammarstrand, "A CPHD filter for tracking with spawning models," *Selected Topics in Signal Processing, IEEE Journal of*, vol. 7, no. 3, pp. 496–507, 2013.
- [14] D. Stoyan, W. S. Kendall, and J. Mecke, *Stochastic geometry and its applications*, 2nd ed. Wiley, Sep. 1995.
- [15] B.-N. Vo, S. Singh, and A. Doucet, "Sequential Monte Carlo methods for Multi-target Filtering with Random Finite Sets," *Aerospace and Electronic Systems, IEEE Transactions on*, vol. 41, no. 4, pp. 1224–1245, Oct. 2005.
- [16] D. Vere-Jones and D. J. Daley, *An Introduction to the Theory of Point Processes*, 2nd ed., ser. Statistical Theory and Methods, D. Vere-Jones and D. J. Daley, Eds. Springer Series in Statistics, 2003, vol. 1.
- [17] E. Delande, M. Uney, J. Houssineau, and D. E. Clark, "Regional Variance for Multi-Object Filtering," *IEEE Transactions on Signal Processing*, vol. 62, no. 13, pp. 3415 – 3428, Jul. 2014.
- [18] S. K. Srinivasan and A. Vijayakumar, *Point Processes and Product Densities*. Alpha Science Int'l Ltd., 2003.
- [19] J. E. Moyal, "The General Theory of Stochastic Population Processes," *Acta Mathematica*, vol. 108, no. 1, pp. 1–31, Dec. 1962.
- [20] H. W. Watson and F. Galton, "On the Probability of the Extinction of Families," *Journal of the Anthropological Institute of Great Britain*, vol. 4, pp. 138–144, 1875.
- [21] P. Bernhard, "Chain differentials with an application to the mathematical fear operator," *Nonlinear Analysis*, vol. 62, pp. 1225–1233, 2005.
- [22] D. E. Clark and J. Houssineau, "Faà di Bruno's formula and spatial cluster modelling," *Spatial Statistics*, vol. 6, pp. 109–117, 2013.
- [23] —, "Faà di Bruno's formula for chain differentials," *arXiv:1310.2833*, 2013.
- [24] F. Faà di Bruno, "Sullo Sviluppo delle Funzioni," *Annali di Scienze Matematiche e Fisiche*, vol. 6, pp. 479–480, 1855.
- [25] D. E. Clark, J. Houssineau, and E. Delande, "A few calculus rules for chain differentials," *arXiv:1506.08626*, 2015.
- [26] S. K. Srinivasan, *Stochastic Point Processes and Their Applications*. Griffin's Statistical Monographs and Courses, 1973.
- [27] B.-T. Vo, B.-N. Vo, and A. Cantoni, "Analytic Implementations of the Cardinalized Probability Hypothesis Density Filter," *Signal Processing, IEEE Transactions on*, vol. 55, pp. 3553–3567, 2007.
- [28] D. Lambert, "Zero-Inflated Poisson Regression, with an Application to Defects in Manufacturing," *Technometrics*, vol. 34, no. 1, pp. 1–14, feb 1992.
- [29] C. A. Charalambides, *Enumerative combinatorics*. CRC Press, 2002.
- [30] D. Cvijović, "New identities for the partial Bell polynomials," *Applied Mathematics Letters*, vol. 24, no. 9, pp. 1544–1547, 2011.
- [31] B.-N. Vo and W.-K. Ma, "The Gaussian Mixture Probability Hypothesis Density Filter," *Signal Processing, IEEE Transactions on*, vol. 54, no. 11, pp. 4091–4104, Nov. 2006.
- [32] D. Schuhmacher, B.-N. Vo, and B.-T. Vo, "A Consistent Metric for Performance Evaluation of Multi-object filters," *Signal Processing, IEEE Transactions on*, vol. 56, no. 8, pp. 3447–3457, Aug. 2008.
- [33] A. L. Gibbs and F. E. Su, "On Choosing and Bounding Probability Metrics," *International Statistical Review*, vol. 70, no. 3, pp. 419–435, 2002.
- [34] D. Vere-Jones and D. J. Daley, *An Introduction to the Theory of Point Processes*, 2nd ed., ser. Statistical Theory and Methods, D. Vere-Jones and D. J. Daley, Eds. Springer Series in Statistics, 2008, vol. 2.